Tangles and cubes for gravity

M. D. Sheppeard

Abstract

In this short note we describe the correspondence between tangles and associahedra tiles, where $\mathbb{R}$ occurs in the case of braid tangles, leading to a natural extension to ribbons for $\mathbb{C}$. Such tangles come from the Temperley-Lieb algebra and were used by Bar-Natan to study Khovanov complexes in nice cobordism categories.

1 Introduction

Khovanov homology [1] for links and tangles was studied by Bar-Natan [2] using a careful construction of cobordism categories. In particular, we do *not* require a tangle diagram to be thought of as a morphism between source and target. For many applications, it is preferable to bound the core of the planar tangle diagram with a polygon with an arbitrary number of sides. Then a trace of the core uses arcs in any number of different directions. Such a trefoil tangle is shown in figure 3.

After Bar-Natan [2], the core of a tangle diagram, which contains all the crossings, will be drawn inside a polygon with B sides. This core diagram meets the boundary polygon in generic points along the edges. Outside the polygon, a set of non crossing loops will join the points on any given edge. Observe how we generalise the use of sources and targets for braid diagrams, corresponding to a polygon with only $B = 2$ sides.

Our motivation is cohomology for motivic gravity [3][4][5], and we will see below that the ubiquitous associahedra are closely related to tangles inside polygons. Both associahedra and cubes appear [6][7][8] in configuration spaces associated to cubics, which are applied to rest masses.

2 Tangle traces

No matter how many sides B our tangle boundary has, on each edge we will place N points. For braid tangles, N can take any value, but for ribbons we set $N = 2m$. A *trace* on such a polygon with B sides is defined to be a selection of non crossing loops between points on the same edge of the polygon, as shown in figures 1 and 2. A *ribbon trace* clearly requires $N = 0 \mod 4$, and there are $2^{m/2-1}$ such diagrams. The total number of braid traces on each edge is 2^{m-1}, which counts noncommutative partitions, shown for $N = 8$ in figure 1.

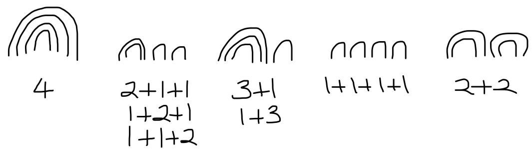

Figure 1: Noncommutative partitions counting traces

When $N = 12$, the ribbon traces of figure 2 reduce the 32 braid traces down to just four. An example of a full ribbon trace is shown for the trefoil knot of figure 3. This diagram is pleasing to physicists, because it replaces a B_2 braid for $B = 2$ with a representation that is truly ternary, reflecting the three dimensions of space [3].

Figure 2: Four ribbon traces at $N = 12$

In analogy to the smoothing cubes in Khovanov homology, the traces on an edge belong to a cube. However, we are more interested in completely general smoothing diagrams, to be used in the basic axioms of categories with more than two arrow ends.

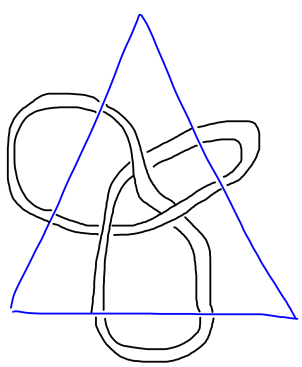

Figure 3: A ribbon trefoil traced on a triangle

3 Loop free smoothings

Let (B, N) denote the space of all possible diagrams on a polygon with B sides, with N points on each edge. The outer traces are described above. Inside the polygon, we permit smoothing diagrams, without specifying a knot or link, and with no internal loops. That is, all possible non crossing diagrams between the boundary points are allowed. Examples are given in figures 4 and 5.

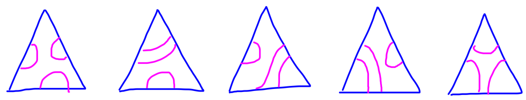

Figure 4: 5 diagrams in $(B, N) = (3, 2)$

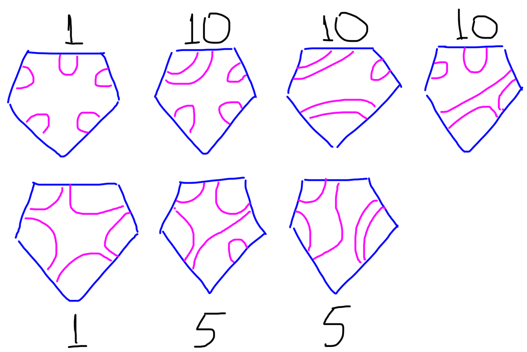

Figure 5: 42 diagrams in $(B, N) = (5, 2)$

The easy proof that $(B, 2)$ contains a Catalan number C_B of smoothings is given in figure 6. Each diagram corresponds to a rooted binary tree vertex on an associahedron [9][10]. The associahedron point is the $B = 1$ trivial polygon, and at $B = 2$ we have the tangle associator edge. These two diagrams also represent four leg trees when a propagator stands in for the area bounded by the two pink edges, as shown in figure 7. Such diagrams form a basis for the Temperley-Lieb algebra in the theory of planar algebras [11][12].

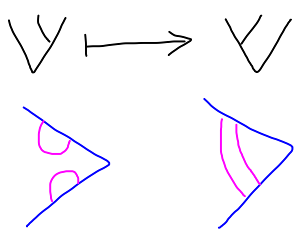

Figure 6: Proof of polygon Catalan numbers

What about higher dimensional faces of the associahedron? The saddle cobordism of figure 7 is the associator edge, modelling edges on associahedra in all dimensions. Since we are secretly talking about homotopy, we go upwards in dimension from there. For us, the dimension of an associahedron polytope is the categorical dimension that we are working in, because particle number must increase with dimension in quantum computation.

Long ago, I forget where, J. Loday pointed out that the trefoil knot could be drawn on the nine faces of the $B = 4$ associahedron. Each crossing is drawn on one of the three square faces, and each pentagon face carries a single arc. To turn our trefoil triangle into this associahedron, we first create a tetrahedron with an unused vertex at infinity, so that each trace arc sits on a triangle face. Now put three vertices right in the centre of the crossing triplet, and two extra vertices along each edge between the ribbon arc ends. Along with our four tetrahedron vertices, and an extra vertex in the centre of the central tetractys, we have the required 14 vertices.

Here the $3+1$ points that are placed inside the crossing triplet resemble the $3+1$ points that are added to the 10 point sheaf cohomology good cover of $\mathbb{RP}^2$, to obtain the associahedron. This is cohomology.

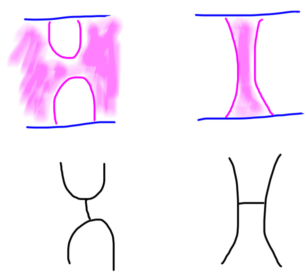

Figure 7: Scattering channels as tangles

4 Comment on gravity

The combinatorics of genus zero moduli spaces with $B + 2$ points is well known to come from the associahedra [7]. In the geometry of line configurations for cubics, both associahedra and cubes are required to tile the S^3 boundary of a 4-cell [8]. Such complex tilings are essential to the Higgs mechanism [6] in the motivic reformulation of the Standard Model, which we already know makes heavy use of the associahedra.

A canonical correspondence between algebraic tangles and polytope axioms is central to the philosophy of the motivic approach, wherein the old *space goes to algebra* functors of topological field theories are replaced by one special infinite dimensional category (or generalised category) that encapsulates the monadicity of quantum logic.

A cube of size $2^{B(m/2-1)}$ is built out of tangle traces. As N increases by one step of 4, this cube grows by a factor of 2^B, which equals 16 in the case of $B = 4$. Such outer cubes describe spinor degrees of freedom [13].

5 Link smoothings

There are 2^n smoothings for an n crossing link. Figure 8 gives 2 smoothings for a single crossing inside a single edge, and 4 smoothings for two crossings inside the two edge polygon.

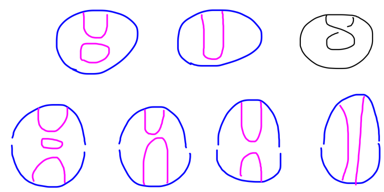

Figure 8: Smoothings for $B = 1$ and $B = 2$

Trefoil knot smoothings are shown in figure 9, along with the sign labels for the vertices of the Khovanov cube. Observe how the Catalan basis is a reduction of the smoothing set to topologically equivalent diagrams, removing internal loops. But the Catalan number C_B is only less than 2^B for $B \in \{1, 2, 3, 4\}$. As C_B grows, more and more general diagrams match zero smoothings.

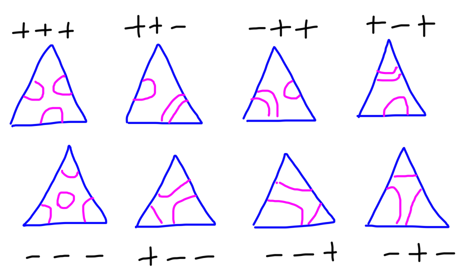

Figure 9: Eight smoothings for the trefoil knot

Figure 10 displays noncommutative partitions of 4 as both trees and signs, where signs mark the areas between leaves. As categorical axioms, such two level trees indicate two composition types: horizontal (at the root) and vertical (central nodes). When each leaf stands for a 2-cell, a tree determines a composition in the 2-category. A smoothing also has a corresponding Tutte contraction, starting with the triangle for the trefoil, and here expressed at level 1 in the trees.

Letting L denote the pruned tree level and d the number of leaves, there are L^{d-1} trees on a subdivided cube diagram. For example, at level 3 there are 9 ways to write lists of noncommutative partitions of 3, ending with $(1, 1, 1)$. Matching integral coordinates, we associate any qudit pure state with a pruned tree, so that pure states in any dimension are precisely the set of all trees.

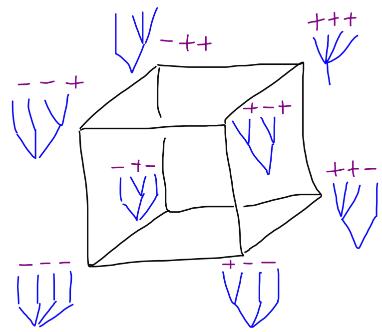

Figure 10: Two level trees as noncommutative partitions

References

[1] M. Khovanov, Duke Math. J. 101 (2000) 359-426

[2] D. Bar-Natan, Geom. Top. 9 (2005) 1443-1499

[3] M. D. Sheppeard, viXra:1909.0428, 2019

[4] M. D. Sheppeard, J. Phys.: Conf. Ser. 1194 (2019) 012097

[5] M. D. Sheppeard, PhD thesis, University of Canterbury, 2007

[6] M. D. Sheppeard, viXra:1910.0263, 2019

[7] M. Yoshida, Kyushu J. Math. 50 (1996) 493-512

[8] J. Sekiguchi and M. Yoshida, Kyushu J. Math. 51 (1997) 297-354

[9] J. D. Stasheff, Trans. Amer. Math. Soc. 108, 293, 1963

[10] T. Leinster, *Higher operads, higher categories*, Cambridge, 2004

[11] V. F. R. Jones, arXiv:math/9909027, 1999

[12] E. Peters, arXiv:0902.1294, 2009

[13] P. Truini, M. Rios and A. Marrani, arXiv:1711.07881, 2017